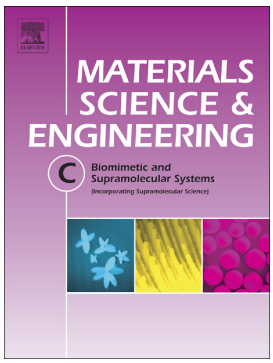

Effect of structure in ionised albumin based nanoparticle: Characterisation, Emodin interaction, and in vitro cytotoxicity

Macarena Siri, Maria Julieta Fernandez Ruocco, Estefanía Achilli, Malvina Pizzuto, Juan F. Delgado, Jean-Marie Ruysschaert, Mariano Grasselli, Silvia del V. Alonso

PII: S0928-4931(19)30546-6
DOI: https://doi.org/10.1016/j.msec.2019.109813
Article Number: 109813
Reference: MSC 109813

To appear in: *Materials Science & Engineering C*

Received date: 12 February 2019
Revised date: 9 May 2019
Accepted date: 27 May 2019

Please cite this article as: M. Siri, M.J.F. Ruocco, E. Achilli, et al., Effect of structure in ionised albumin based nanoparticle: Characterisation, Emodin interaction, and in vitro cytotoxicity, Materials Science & Engineering C, https://doi.org/10.1016/j.msec.2019.109813

Effect of structure in ionised albumin based nanoparticle: Characterisation, Emodin interaction, and *in vitro* cytotoxicity.

Macarena Siri[1], Maria Julieta Fernandez Ruocco [1,3], Estefanía Achilli[2], Malvina Pizzuto[4, *], Juan F. Delgado[5], Jean-Marie Ruysschaert[4], Mariano Grasselli[2], Silvia del V. Alonso[1,+]

[1]Laboratorio de Biomembranas (LBM), Departamento de Ciencia y Tecnología, Universidad Nacional de Quilmes, IMBICE-CONICET-CICPBA
[2]Laboratorio de Materiales Biotecnológicos (LaMaBio), Departamento de Ciencia y Tecnología, Universidad Nacional de Quilmes, IMBICE-CONICET-CICPBA
[3]Instituto de Biofísica Carlos Chagas Filho, Universidade Federal do Rio de Janeiro, Brazil.
[4]Laboratory of the Structure and Function of Biological Membranes, Center for Structural Biology and Bioinformatics, Université Libre de Bruxelles, CP 206/02, Bd du Triomphe, 1050 Brussels, Belgium
[5]Laboratorio de Obtención, Modificación, Caracterización y Evaluación de Materiales (LOMCEM), Conicet, Universidad Nacional de Quilmes.

+Corresponding author: Silvia del Valle Alonso
Departamento de Ciencia Y Tecnología
Universidad Nacional de Quilmes
IMBICE - CONICET
Roque Saenz Peña 352
(B1876BXD) Bernal, Buenos Aires, Argentina
TE: +54 43657100 ext. 5625
FAX: +54 4365 7132
salonso@unq.edu.ar

Author Contributions

The manuscript was written through the contributions of all authors. All authors have approved the final version of the manuscript.

* Current address: Molecular inflammation group, Biomedical Research Institute of Murcia, Clinical University Hospital Virgen de la Arrixaca, IMIB-Arrixaca, Carretera Buenavista s/n. 30120 Murcia, Spain.

Abstract

A γ–irradiated bovine albumin serum-based nanoparticle was characterised structurally, and functionally. The nanoparticle was characterised by A.F.M, D.L.S, zeta potential, T.E.M., gel-electrophoresis, and spectroscopy. We studied the stability of the nanoparticle at different pH values and against time, by fluorescence spectroscopy following the changes in the tryptophan environment in the nanoparticle. The nanoparticle was also functionalized with Folic Acid, its function as a nanovehicle was evaluated through its interaction with the hydrophobic drug Emodin. The binding and kinetic properties of the obtained complex were evaluated by biophysical methods as well as its toxicity in tumour cells.

According to its biophysics, the nanoparticle is a spherical nanosized vehicle with a hydrodynamic diameter of 70 nm. Data obtained describe the nanoparticle as nontoxic for cancer cell lines. When combined with Emodin, the nanoparticle proved to be more active on MCF-7 cancer cell lines than the nanoparticle without Emodin.

Significantly, the albumin aggregate preserves the main activity-function of albumin and improved characteristics as an excellent carrier of molecules. More than carrier properties, the nanoparticle alone induced an immune response in macrophages which may be advantageous in vaccine and cancer therapy formulation.

Keywords: Bovine Serum Albumin (BSA), BSA-nanoparticle (BSA NP), Emodin, drug delivery.

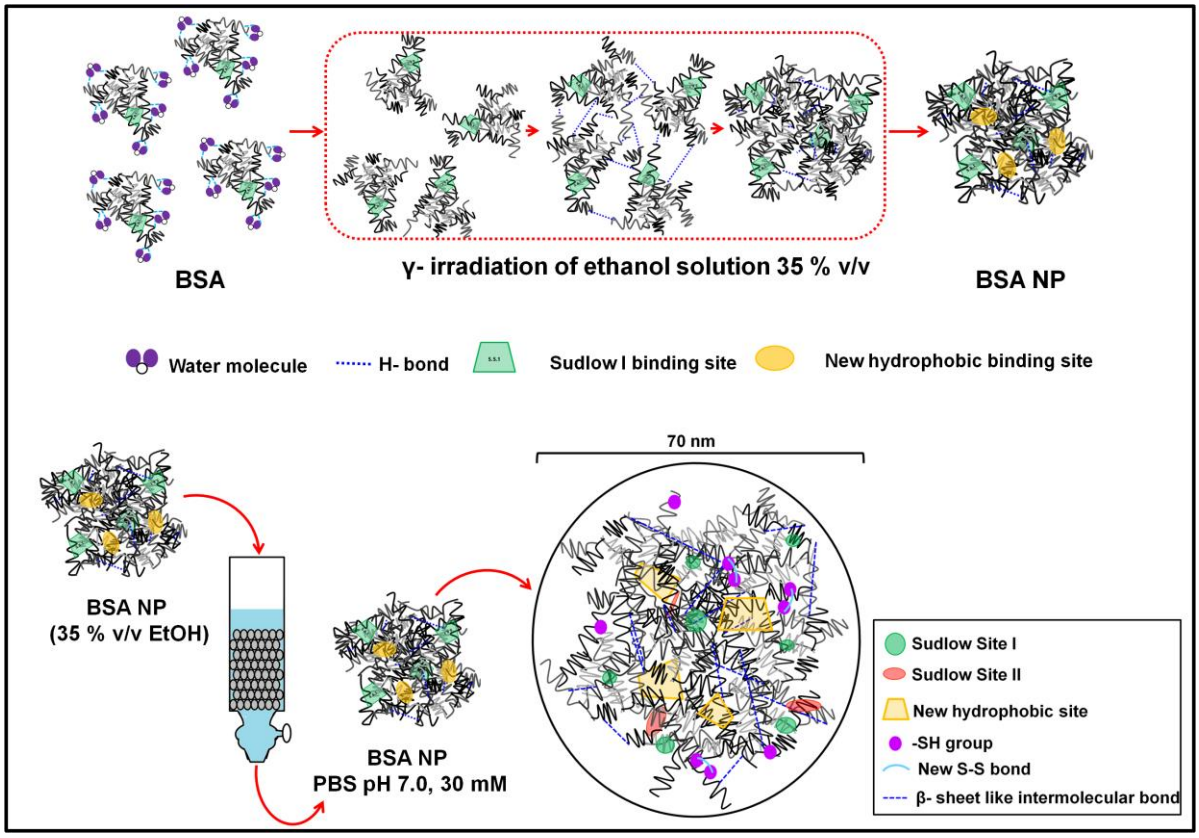

Graphical Abstract

Introduction

Protein-based nanoparticles constitute an alternative to classical protein-ligand complexes as drug delivery systems. They also display interesting biophysical and functional properties based on multi-site localised specific binding sites of the protein surface [1].

When designing and preparing a protein nanoparticle (NP), the preservation of its primary function is highly essential. The challenge is not to let the preparation method influence the primary function of the protein, despite any small change in the molecule's secondary structure. Proteins forming part of the NP can face substantial challenges to their activity due to structural alteration during the NP preparation process. If the alteration results in loss of functionality, then future protein modification might be required. However, if the NP is designed in the right way, it could significantly enhance the delivery of the desired substance [2]. Current techniques based mainly on chemical methods are employed for the synthesis of protein nanoparticles [3]. A highlighted feature of proteins is their capacity to aggregate in a size-dependent manner according to the concentration of ethanol used. The aggregation eases the tailoring to desirable functional size-stable NPs for *in vivo* penetration. The preparation methods in ethanol solution and lyophilisation of the BSA NP were published in previous works [3][4][5]. In this structural study, we give a complete biophysical characterisation of the gamma-irradiated albumin-based nanoparticle, where DLS size and microscopy was covered before [4]. Structural and functional studies are given in order to propose the nanoparticle as a suitable drug delivery system. As BSA is known as an excellent carrier for drugs, it is expected that the NP should be able to bind to antitumor drugs. In our work, we succeeded in preparing an NP by using γ irradiation as a crosslinker in order to avoid residual toxic organic secondary products and help control the size protein NP as clean as possible [3][6].

The study aims to characterise a bovine serum albumin nanoparticle (BSA NP). This nanoparticle presents the advantage of only having BSA in its composition thanks to the gamma irradiation process. If the nanoparticle is non-toxic, its potential as a as drug delivery system will escalate[3][4][10]. The stability experiments at different pHs and chaotropics were carried out mainly by fluorescence spectroscopy.

In some cases, the findings of the NP behaviour were contrasted with albumin. We also aim at the biophysical characterisation of the NP bioconjugate Emodin (E) / BSA NP (BSA NPE) as a drug delivery system. As a result, a confirmation of a stable, non-toxic NP with small structural changes was obtained. The toxicity effect *in vitro* in cell lines like MCF7 and PC3 was evaluated on the free drug, free NP and the bioconjugate BSA NPE. The ability of BSA and BSA NP to induce an immune response was evaluated by the quantification of Nuclear Factor – κB (NF-κB) activation in macrophages. NF-κB is a transcription factor whose activation triggers the production of pro-inflammatory cytokines that amplify the innate immune response to bacteria and virus[11]. The results presented here will help understand the nanoparticles–protein-based drug interactions and the role that BSA nanoparticles may play in future biomedical and pharmacological applications.

The drug used in our work is emodin (3-methyl-1,6,8-trihydroxyanthraquinone). The drug is an

orange natural anthraquinone that has been commonly used for its anti-inflammatory and laxative effect. Emodin (E) is a molecule with a structure similar to the anthracene, which has shown in recent years an antitumor effect. It features as an antitumor drug, producing apoptosis by the caspases way in cell lines derived from tumours such as HL60 [2] and HeLa [12][13][14]. It presents an acid-alkaline equilibrium in aqueous solutions, varying back and forth from neutral species, monoanionic and dianionic species [7][9]. As it is, this drug has been studied in recent years because of its many properties, attempts have been made to diminish its secondary effects by different drug delivery systems [4][15][15]. The most important feature of E is the ability to bind to proteins forming complexes. Hence, the reason for choosing the drug in this study [2][9].

2. Experimental Section

2.1. Materials

BSA was purchased from Sigma-Aldrich (A7906-100G Lot SLBC371V), 98% agarose gel electrophoresis, lyophilised powder (Buenos Aires, Argentina). Ethanol was purchased from Biopack (Zarate, Buenos Aires, Argentina) and acetone was obtained from Anedra (Research AG, Tigre, Buenos Aires, Argentina). Sephadex G-200 column for chromatography was obtained from Pharmacia Fine Chemicals (New Jersey, United States of America). Centrifugation tubes were Amicon Ultra, Centrifugal Filtres – 0.5 ml 3K, Ultracel- 30 kDa Membranes from Merck Millipore Corporation (Darmstadt, Germany). Urea was purchased from MERCK (Darmstadt, Alemania), SDS was purchased from Anedra-Research AG (Tigre, Buenos Aires, Argentina) and Tween 80% from FLUKA (Sigma-Aldrich- Buenos Aires, Argentina). All corresponding buffers were PBS analytical grade made.

2.2. Nanoparticle preparation

BSA nanoparticles (BSA NP) were obtained by gamma irradiation according to Soto Espinoza et al., 2012 [3]. The solution in which the BSA NP was obtained was a buffer/ ethanol solution. The buffer corresponded to 30 mM phosphate buffer solution (PBS) at pH 7.0, and the ethanol concentration was 35 % v/v.

Briefly, BSA molecules in a buffer/ ethanol solution were gamma irradiated by a ^{60}Co source (at PISI CNEA-Ezeiza, Argentina), at a dose rate of 1 kGy/h (lowest dose set at two kGy and upper limit dose set at 10 kGy). The sample temperature during irradiation was between 5-10 ºC. After, samples were eluted in a molecular exclusion column to exchange the ethanol solution for 30 mM PBS pH 7.

2.3 Nanoparticle characterisation

All experiments were referred to BSA (MW 66 kDa) of an initial concentration of 4.5 to 450 µM, which corresponds to concentrations of nanoparticle between 5.5 nM to 555 nM. The following concentrations were calculated based on the BSA NP molecular weight (MW 148 MDa) obtained from TEM (spherical shaped NPs) and DLS nanoparticle size of 70 nm. The DLS and Zeta Potential measures were taken with 90 Plus/Bi-MAS particle size analyser as in Siri et al. 2016 [5]. Nanoparticle tracking analysis (NTA) was used for the determination of the number of albumin nanoparticles, in a LM20 instrument (NanoSight, Amesbury, UK) equipped with a 532 nm laser. With this technique we obtained nanoparticle concentration (particle/mL). a BSA NP solution of 0.055 nM was injected into the sample chamber with sterile syringes until the liquidfilled the tip of the syringe (n=3). The final concentration of nanoparticle was calculated using Avogadro´s number. In order to see protein degradation, we considered the BSA NP solution of 0.055 nM as 100 %, and the experimental BSA NP concentration as the real nanoparticle concentration.

2.3.1. Size molecular exclusion

BSA NP was purified by size exclusion chromatography using a Sephadex G-200 column. Eluted fractions were followed by UV-Vis (λ= 280 nm). The hydrodynamic size of the eluted peak was determined through Dynamic Light Scattering analyses.

2.3.2. SDS – PAGE

Different BSA NP obtained from different processes were tested in an SDS- PAGE. A total of 30 µl of each BSA NP were diluted in distilled water and 10 µl of sample buffer reaching a final concentration of 5 µM of protein. Samples were heated up for 5 minutes. Aliquots of 18 µl of sample and protein markers were loaded on an 8 % polyacrylamide gel and 5 % stacking gel. A Biopack Electrophoresis Unit was used to run the SDS – PAGE at a constant voltage of 8 mA. After, the gel was stained using Coomassie blue. For gel analysis, ImageJ Gel Analyses was used.

2.3.3. Transmission electron microscopy (T.E.M)

A Philips high-resolution transmission electron microscopy EM 10A/B 60 KV was used for sample morphology observation. The BSA NP buffer solution was diluted 1/100 for this study (final concentration of 5 nM). Samples were stained with uranyl acetate before the micrographs. A total of 20 microscopies was taken over different fields of the sample. The NP selection was carried out by identification of them based on round shape and definition of the software for analysis used was ImageJ (Fiji). A counting tool from the software was used in order to count the NP in the micrographs and then the profile plot tool was used to describe the size of each NP found.

2.3.4. Atomic force microscopy (A.F.M.)

The BSA NP sample was purified by exclusion chromatography in PBS. A total of 20 µl of the samples were deposited on freshly cleaved mica. After, it was dried for 10 min with nitrogen flux. Images were obtained using a Dimension Icon in Peak Force QNM (PFQNM) (Bruker®). Measures were made with rectangular silicon tip with a nominal spring constant 42 N/m and tip radius of 12 nm. This microscopy took place in the Institute of Biophysics, Universidade Federal do Rio de Janeiro, Rio de Janeiro, Brazil.

2.3.5. UV- Vis spectrophotometry

The absorbance profile of the BSA NP was measured in a Nano-Drop 1000 Thermo Scientific spectrophotometer, with a path length of 0.1 cm. Samples were diluted to a concentration of 5.5 nM in 30 mM PBS (pH 7. 0). A total of 4 µl of each sample was needed for the measure. The profiles obtained went from 240 – 400 nm. Plotting of the measurements and data analysis were done using GraphPad Prism v.5.

2.3.6. Fluorescence spectrophotometry

The fluorescence emission profile of the BSA NP was measured in an S2 Scinco Fluorspectrophotometer. The excitation and emission slits were open at a 1.5 nm distance. BSA NP samples (18 nM) were excited at a wavelength of 295 nm, where emission range was 300 - 400 nm. An ml per sample in 30 mM PBS (pH 7.0) was used in the measurements. Plotting of

the measurements and data analysis were done using GraphPad Prism v.5.

2.3.7. Circular Dichroism (C.D.)

The CD profile of the BSA NP was measured in a Jasco 810 spectropolarimeter equipped with a Peltier cell device for temperature control (Jasco Corporation, Japan), at room temperature with near and far dichroic signal range (240 – 400 nm and 180 – 280 nm, respectively). A quartz cell of 500 µl was needed for the experiment. Concentrations varied according to the signal range desired to record: for the near – CD BSA NP (555 nM), for the far-CD BSA NP (37 nM). Resolution of the samples was of 0.1 nm. Plotting of the measurements and data analysis were done using GraphPad Prism v.5.

2.3.8. FT-IR Spectroscopy

The infrared profile of the BSA NP was measured in an FT-IR Affinity1-Shimadzu ATR with a laser lamp with an absorbance HAPP-GENZEL of 324. Measurements ran wavelength from 400 to 4000 cm^{-1}, with 80 scans per sample and a resolution of 1 cm^{-1}. The cell needed, was of SeZn with 45º of inclination.

Samples were blown-dried until a film was formed to obtain the BSA NP spectrum free of IR-water peaks with The concentration of the sample was 55 nM. The blank was subtracted by software. The spectra were processed, deconvoluted, analysed and the second derivative was obtained with the IR-Solution software (v. 1.50), provided by the manufacturer, and by Prism GraphPad v.5.

2.3.9. Free thiols groups' detection

Samples of BSA NP were diluted 1/10 to a concentration of 0.55 µM for the experiment. The experimental conditions were carried out as described in Grassetti et al., 1967 [6] and modified as in Achilli et al., 2015 [4]. Briefly, the absorbance of the sample at 280 nm was measured. A solution of Ellman's reagent (DTNB) 0.1 M PBS at a 3.9 mg/ml concentration was added to each sample. The incubation lasted for 15 minutes, and then the absorbance at 425 mn was measured again. In order to know how many free thiols we had per NP, we followed the equation,

$$n = (Abs_{DTNB}425nm - Abs_{BLANK}425nm / \varepsilon_{DTNB}425nm)\ 1/CNP$$

where n is the number of moles of thiols per BSA NP, and $\varepsilon_{DTNB}425nm$ is 12400 (mol cm^{-1}). CNP represents the concentration of BSA NP in the sample.

2.3.10. Free amino group's detection

Solutions of BSA NP (18 nM) were used for these measurements. Experimental protocol followed Habeeb et al., 1966 [17] method for free amino determination. Briefly, to an ml of sample was added 1 ml of 4% NaHCO3, pH 8.5 and 1 ml of 0.1 % TNBS. Then, it was incubated for two hours at 42 ºC, in the dark. After, 1 ml of 10 % SDS was added to make the NP soluble together with 500 µl of 1N HCl to prevent its precipitation. Samples were measured before and after treatment for its absorbance at 335 nm.

The ratio between TNBS and BSA NP was estimated as [TNBS]/ [BSA NP]. In order to know the TNBS concentration in the sample, a calibration curve was done.

2.3.11. Determination of surface carbonyl groups (protein oxidation)

Solutions of BSA NP (55 nM) were used in this experiment. The procedure followed Brady's reaction protocol [18]. Briefly, 800 µl of 10 mM DNP in 2 M HCl was added to 200 µl of BSA NP. The incubation lasted an hour at room temperature and in the dark. Every 15 minutes samples were vortexed to promote mixing between the solutions. After incubation finished, an ml of 20 % w/v of TCA was added, and samples were then incubated for 5 minutes in ice. Once incubation finished, the samples were centrifugated at 10000 g at 4 ºC. The pellet from the centrifugation was resuspended in 500 µl of 6 M guanidine. Another centrifugation at 4 ºC for 10 minutes (10000 g) took place before measuring the samples by UV-vis absorbance at 370 nm. For the calculation on the ratio carbonyl groups/ NP, the same steps from 2.4.10 were performed.

2.3.12. Thermogravimetric Analysis (TGA)

BSA NP and BSA samples in miliQ aqueous solution were normalised to an absorbance of 0.371 for this experiment. Samples were lyophilised overnight in order to eliminate any trace of water for the experiment as described in Siri et al., 2016 [5]. Approximately 4 mg of each sample was placed in sample pan and submitted to a heating ramp from 30 °C to 920 °C at 10 °C min-1 in a thermogravimetric balance (TA Q500, TA Instruments, United States). The gas used in the sample was air at 40 mL min-1 and nitrogen at 60 mL min-1 as balance gas. Weight percentage was registered in the function of temperature. From original data, derivative of weight concerning temperature and temperature at 5% weight loss (T95) were calculated. Three independent samples of BSA NP and BSA were analysed.

2.4. Folic Acid attachment to the BSA NP

The folic acid attachment was carried out as described in Du et al., 2013 [20]. Briefly, a 5 mg/ml folic acid solution (FA) with 3 mg of 1-ethyl3-(3-dimethyl aminopropyl) carbodiimide and 2 mg of N-hydroxy-succinimide was kept under constant stirring in the dark at room temperature. Incubation lasted 4 hours. After, a 30 mg/ml BSA pH 7.0 solution was added for every ml of the FA solution. This solution was kept under dark at room temperature overnight.

The FA-BSA was separated from free FA by centrifugation in an ad hoc column of 1 ml Sephadex G50 at 2000 rpm for 2 minutes at 4 °C. An ethanol BSA solution was added to the FA-BSA solution until reaching 35 % v/v of ethanol in the solution composition. The solution as it was gamma irradiated by a 60Co source (at PISI CNEA-Ezeiza, Argentina), at a dose rate of 1 kGy/h (lowest dose set at 2 kGy and upper limit dose set at 10 kGy). The sample temperature during irradiation was between 5-10 ºC. After, samples were eluted in a molecular exclusion column to exchange the ethanol solution for 30 mM PBS pH 7.

In order to estímate the process yield, samples were measured for its UV-visible absorbance at 363 nm. The spectrum represents the FA absorbance maximum, which allowed the quantification of the FA attached to the nanoparticle.

The folic acid attachment was carried out as described here and after the irradiation of the BSA NP. Both products were analysed and compared.

2.4.1. Interaction study: FA-BSA NP with Emodin (E)

For this study, 18.4 nM of FA-BSA NP dispersion was used together with a 450 µM emodin (E) ethanol solution. Dilutions on the E solution were made in order to follow an [E]/[FA-BSA NP] ratio range between 0.00 – 12000, where the E highest final concentration used was 90 µM. The determination of the dissociation constant (Kd) was carried out as explained in Sevilla et al., 2007 [9].

2.4.2. A cytotoxicity study in MCF-7 cells treated with FA-BSA NP

The functionality of the FA-BSA NP and the bioconjugate FA-BSA NP/E was evaluated through a metabolic activity assay in the human tumour breast cell line MCF-7. Cells were kept at 37 °C with a 0.5 % CO2 injection with MEM media, 10 % v/v fetal bovine sera.

The assay was carried out through the reduction of tetrazolium dye MTT 3-(4,5-dimethylthiazol-2-yl)-2,5-diphenyltetrazolium bromide to its insoluble formazan form. Cells in a 96 well plate were incubated with 55 nM FA-BSA NP and 45 µM E solutions for 4, 24 and 48 hours (groups of n=12). After incubation, 100 µl of a 1/ 10 of 2 mg/ml MTT solution was added to each well. After 45 minutes incubation, the plate was incubated with 200 µl DMSO/ well, and the well absorbance was measured at 590 nm. Control cells were those with no treatment. Thus they represent 100 % of metabolic activity. Results represent triplicates of the assay.

2.6. Cell immune activation by NPs

The samples studied in this section were increasing concentrations of BSA; BSA NP; lyophilised BSA NP in PBS 30 mM, pH 7.0 and FA-BSA NP.

2.6.1. Murine RAW-BLUE immune response

Raw-Blue™ cells were cultured in DMEM supplemented with 10% heat-inactivated FBS from South America, 2 mM L-glutamine, 1 mM sodium pyruvate, 50 U/ml penicillin, 50 µg/ml streptomycin and 200 µg/ml Zeocin. All cells were maintained at 37°C in a 5% CO2 atmosphere.

RAW-Blue™ cells (RRID:CVCL_X594), Zeocin™ and Quanti-Blue™ were from InvivoGen. DMEM (Dulbecco's Modified Eagle's Medium) media, L-glutamine, sodium pyruvate, penicillin, streptomycin and Fetal bovine serum (FBS) from South America were from Lonza.

The cell line was tested for mycoplasma contamination on a regular basis. To avoid divergence from the parent line, cell cultures were passaged up to 10 times.

As donde before, 250000 RAW-Blue cells per well were seeded in a 48 well plate, 24 hours before the experiment [10]. Incubation with the samples lasted 22 hours, where samples were diluted in complete media (DMEM+FBS 10%). At the end of each incubation, the supernatant was removed and preserved for future NF- κB activation/Quanti-Blue assay. Cells incubated in

complete media without stimulant served as negative control.

2.6.2. Cell Metabolic Activity Experiment

Briefly, after 2 hours of incubation at 37 °C, 5 % CO2, the plate was centrifuged, the media removed, and 150 µl of DMSO was added per well. The plate was read in a BioTek plate reader at 570 nm and 620 nm as reference wavelength.

2.6.3. NF-κB activation

NF-κB activation was evaluated by measuring the NF-κB-dependent alkaline phosphatase (SEAP) secreted by RAW-Blue cells in the collected supernatants by using the Quanti Blue™ reagent (InvivoGen), according to manufacturer's instructions. Absorbances were read with a BioTek Synergy HT Microplate Readers.

Data were normalised to the value of cells without any stimulant and represented by Software Excel v. 2015.

3. Results and Discussion

3.1 Size exclusion chromatography and SDS gel electrophoresis

Nanoparticles formed from BSA molecules (BSA NP) by desolvation in an ethanol solution were then stabilised by γ irradiation [3][4][5] (Figure 1a). After the preparation process, the NPs were separated by a size exclusion chromatography column (Sephadex G – 200) into different populations according to the order of elution; those of a larger size eluted first, followed by the smaller population (Figure 1b). The aliquots were then identified by UV-Vis spectroscopy: the first maximum was identified as NP, while the second maximum was identified as residuary albumin. According to the elution profile, the colloidal solution contained 80 % NP and 20 % of residuary free BSA molecules (Figure 1b).

An SDS- PAGE gel was run in order to study the BSA NP assembly (Figure 1c). If weakly linked proteins form the NP, the mild denaturation experimental conditions in which the gel is carried out (SDS presence in gel) would be enough to disaggregate the BSA NP. Contrary to this, if strong forces crosslinked the BSAs, then the NP will not run, offering a distinguishable one spot protein aggregate in the stacking gel. Neither condition is desirable; the BSA NP should have stability balanced between both extremes, as it must preserve its function as a carrier for a drug and biodegradability after delivering the drug.

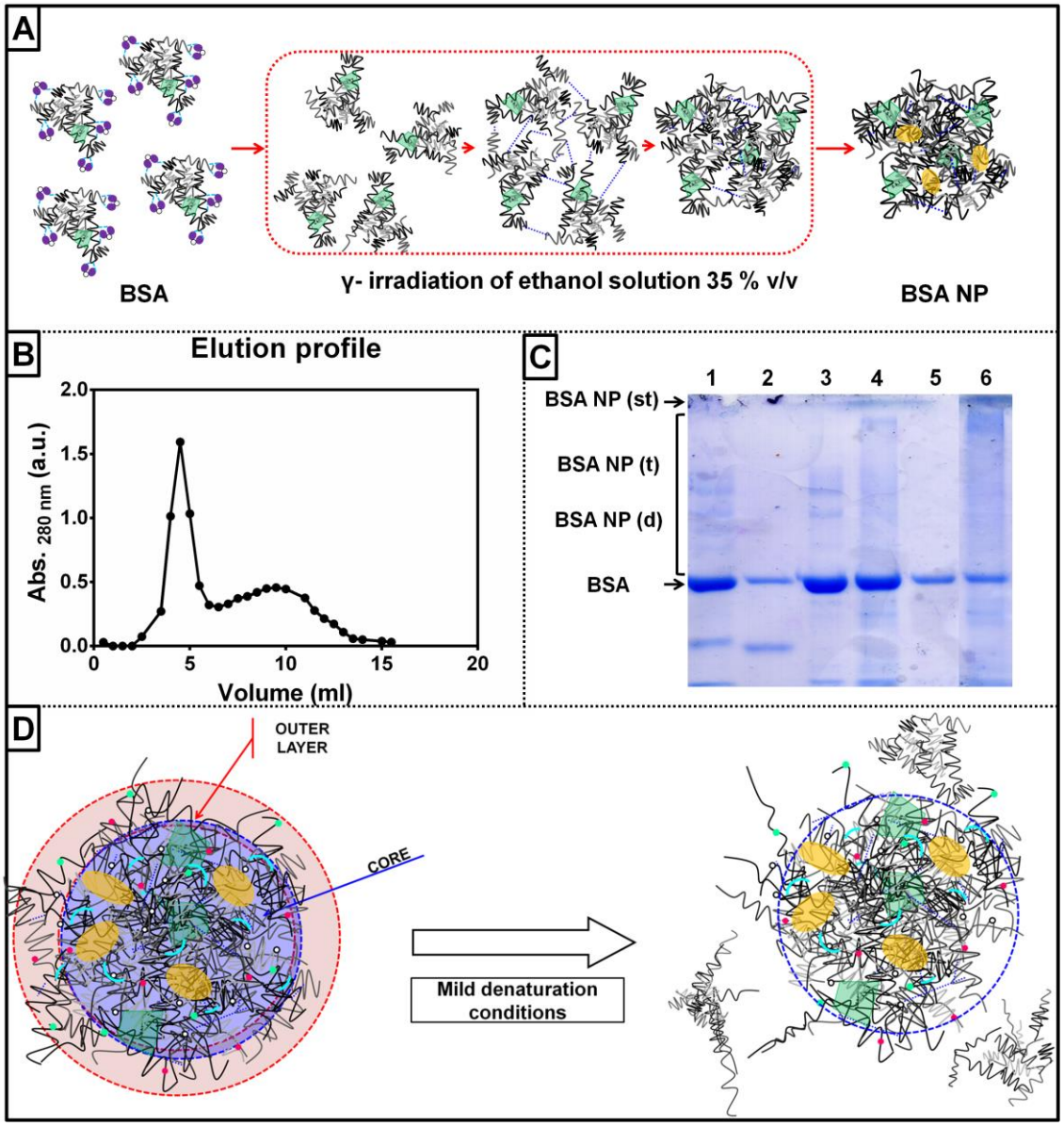

Figure 1. (a) Illustration of the process of irradiation by which the BSA NP is obtained. (b) Elution profile obtained from a size exclusion column of the BSA NP. (c) SDS- PAGE of BSA NP samples; 1) protein molecular markers (BSA trimers, dimers and monomers), 2) protein molecular markers (BSA, ovalbumin, lysozyme – not visible in gel), 3) BSA in buffer PBS 30 mM, pH 7.0, 4) BSA NP in ethanol solution 30 % v/v, 5) BSA NP in buffer PBS 30 mM, pH 7.0, 6) BSA NP after separation in a G200 Sephadex size exclusion chromatography column. (d) Illustration of the BSA NP outer layer and core with different forces involved in each section according to results in Figure 1 (c).

The assembly of the NP was tested in different conditions (Figure 1c).

It was possible to observe different aggregate sizes in each sample. All lanes showed different concentrations of free BSA (66 kDa). The stacking gel showed stains belonging to NP that did not run in every lane. BSA NP Sephadex G200 (Figure 1c, lane Nº 6), was the sample with the highest concentration of NP; 68 % of NP distributed; 48 % in the stacking gel and 20 % of different NP sizes. This NP was also the one with the least concentration of free BSA (31 %). The rest of the BSA NP samples showed a higher concentration of free BSA, (30 - 80 %) and an

NP concentration ranging from 8 to 30 % (Figure 1c). Because of the profile of the running gel, it is suggested that different forces assemble the BSA NPs. When subjected to mild adverse experimental conditions, like an SDS-PAGE, the NP would lose some of the attached BSA molecules in its composition. The lost molecules represent the weakly external linked layer (Figure 1d). As none of the BSA NP samples, except for BSA NP Sephadex G200, was separated from the residuary protein after irradiation, they showed a large percentage of free BSA (Figure 1c). As a result, the weakly linked BSA molecules in the NP joined the residuary BSA in the sample (20%), resulting in a higher percentage of free BSA (over 20%). This weakly linked protein layer could be described as an external layer protecting a deeper albumin core where the protein molecules were crosslinked by stronger forces that are difficult to destabilise. The different bands observed in every lane seeded with BSA NP are also indicative of the presence of different NP sizes resulting from the NP degradation (Figure 1d).

3.2 Structure, morphology and size

The size of the NP obtained was of 70 nm of diameter and a Zeta potential value of -25 mV confirming data previously reported [5]. According to T.E.M, the BSA NP has a spherical-like shape with a given mean diameter of 35 nm (Figure 2a-b). The results represent a monomodal population with a minor polydispersity (35.4 ± 0.35 nm) (Figure 2c). The microscopy also shows aggregation of the sample (Figure 2a-b). This aggregation could be because of the dehydration the sample undergoes during experimental preparation. NTA results showed a BSA NP concentration of 2.93 $x10^{13}$ particle/ml ± 1.96 $x10^{12}$ particle/ml in its main population (c.a. 100 nm ± 30 nm) which means an actual nanoparticle concentration of 90% from the initial protein concentration. Therefore, the gamma irradiation process for nanoparticle obtention means minimal protein degradation compared to albumin NP prepared by desolvation methods [21]. Study also shows less than 20 % of nanoparticle aggregation.

The A.F.M showed aggregation of the BSA NP in the dehydrated state, together with BSA molecules in the background (Figure 2d). A magnification of a single BSA NP particle showed defined edges and heterogeneous surface (Figure 2e). The height of the NP obtained in the microscopy corresponds to 64 nm, which is within the average measurements for the BSA NP obtained by D.L.S measurements [5].

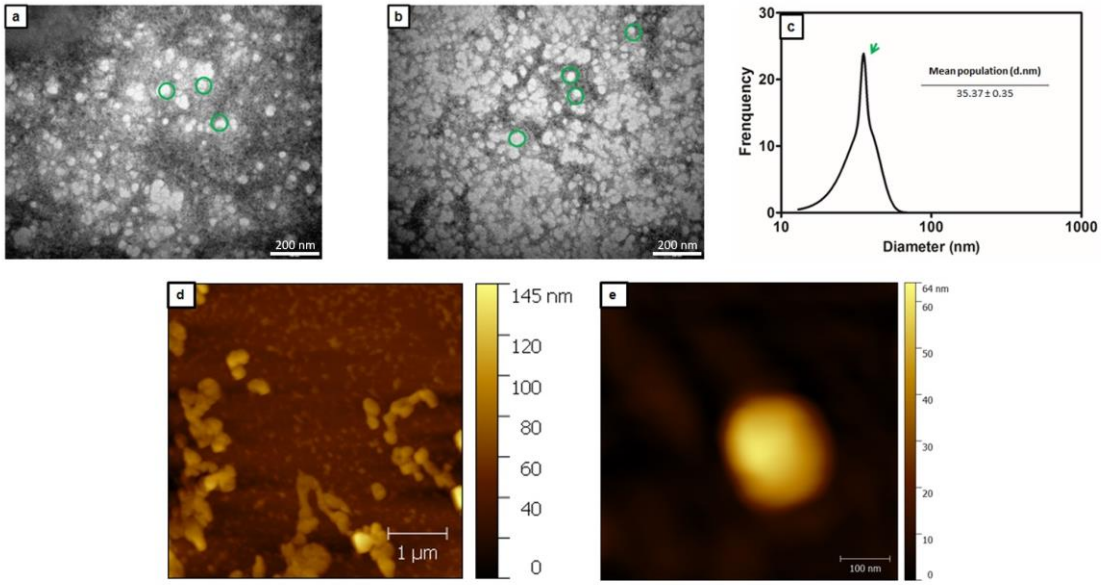

Figure 2. Transmission electron microscopy (T.E.M) of the BSA NP (a-b). Microscopies represent different samples fields were the magnification correspond to 50.000 X, were 1 cm= 200 nm. 20 microscopies were taken, and a total of 450 NP were counted. (c) T.E.M histogram represents the mean size of the total of NP analysed. Atomic Force Microscopy (A.F.M.) of the BSA NP (d-e) Microscopies represents the aggregation in the sample while dehydrated state for A.F.M. (d). Magnified single BSA NP (e).

As stated before, according to the TEM taken, the NP's diameter resulted in approximately 35 nm, which coincides with our previous results in an ethanol buffer solution in the range 20 - 40 nm [3]. The differences among the NP sizes obtained using different techniques are because: BSA NP for TEM and BSA NP in ethanol solution provide a dehydrated state; in a buffer solution, the NP is hydrated, therefore its diameter varies into 70 nm. According to these parameters, each NP is formed by 2246 BSA molecules. The diameter of the NP implies that as a carrier the ratio between volume and surface is optimised; the surface tension is reduced. Its shape would allow a better circulation if IV administered; therefore, the NP will be able to avoid attachment to the vessels [14].

AFM showed that the BSA NP has an ellipsoidal shape and irregular surface. The albumin does not have a smooth surface. During the NP preparation process, the protein molecules may have suffered some degradation and structure alteration typical due to the steps involved in the preparation process (ethanol desolvation and gamma irradiation). Hence, the irregular surface feature of the NP is corroborated (Figure 2d-e).

3.3. Spectroscopy methods

Detecting any alteration in the BSA molecules forming the NP might imply an overall loss of function. The preservation of function in the BSA NP is essential as it is aimed at improving drug delivery in medical treatments.

Unlike albumin UV-vis spectra (shoulder at 283 nm), the UV-Vis profile of BSA NP shows the $Trp_{BSA\ NP}$ shoulder at 277 nm and a shoulder broadening of 7 nm (from 18 to 25 nm)(Figure 3a). According to Rohiwal et al., 2016 [22] a broadening of the shoulder in the BSA NP spectra

means not only conformational alterations in the structure of the proteins forming the NP but an alteration in size of the particle in the colloidal suspension (Figure 3a). The alteration in size was expected as now the solution contains nanoparticles formed by the protein molecules. Further spectroscopic experiments were carried out in order to elucidate these alterations in structure.

The BSA NP FT-IR spectra showed that the 1652 cm^{-1} maximum representing the α-helix composition of the protein did not experience any displacement during NP formation (Figure 3b). This maximum is of great importance as it is sensible to the environment and any change in the protein structure. The alpha - helix content, the most critical domain in the secondary structure of the protein, is not lost. The band corresponding to β-sheet structure signal (1510 – 1545 cm^{-1}) is present in the NP profile, whereas this maximum is absent in the BSA profile (Figure 3b).

From this and the UV –visible data, we state that when forming the NP, the dehydration of the BSA molecule is significant enough to bring the molecules together in an attempt to compensate for the H-bonding loss in the absence of water by the desolvation process. These bonds help maintain the β-sheet structure: the BSA NP spectra showed less CO, CN and NH groups' freedom degrees (groups prone candidates to this kind of structures). The fact that there is also a frequency displacement of the carbonyl groups that do not accept H bonding, from 1600 cm^{-1} to 1555 cm^{-1}, means that the NP has a more compact structure than BSA [22].

We observed by fluorescence spectroscopy that the BSA NP fluorescence profile showed a slight displacement of 2.5 nm to lower wavelength (blue shift) meaning a more hydrophobic $Trp_{BSA\ NP}$ environment, confirming UV-visible data (Figure 3c). The spectra showed a slight emission decrease in the $Trp_{BSA\ NP}$, describing a possible quenching effect among the various Trps present in the BSA NP due to molecular crowding forming the NP [5]; the Trps (143 and 212) are closer to each other, generating a quenching effect (Figure 3c). This quenching suggests that the albumin forming the BSA NP has a more compact conformation than free BSA.

The C.D. spectra from BSA NP showed aggregation of the molecules forming the NP in the secondary structure in both near and far CD (Figure 3d-e). The aromatic peaks in the near – CD gave a low signal in the BSA NP spectrum (Figure 3d). The same was observed in the α-helix and β- sheet peaks in the far – CD (Figure 3e). Both results are indicative of structural alteration in the BSA molecules described as protein aggregation.

The methodologies used as γ irradiation are expected to generate surface modifications of the functional groups present in the surface of the NP due to ROS formation. Detecting the presence of these groups is useful for describing how the BSA molecules are bonded between each other, or any other alteration structure. Experiments were carried out to detect how many –SH, -NH and –CO superficial groups the BSA NP has.

In the second derivative of the spectra, some changes were observed in the amide zone, generally attributed to conformational changes (Figure 4) [23]. In the spectra of BSA, a peak was observed at 1627 - 1625 cm-1 which was moved to 1619 cm-1 in nanoparticle state. Lu et al. (2014)[23] studied the denaturation of the BSA by heat used D2O and attributed the bands,

according to the criterion of the second derivative, 1632 - 1638 cm-1 to short-segment chains connecting the α-helical segment and 1610 -1620 cm-1 to the intermolecular β-sheet structure. The band at 1650 cm-1 was not modified, and this was previously assigned to α-helix structure (1653 cm-1). In the nanoparticle state, it seems to induce changes in the conformation of the BSA protein.

Results showed a considerable amount of the three mentioned surface groups present in the NP (Figure 3f). According to the increased number of functional groups in BSA NP, the differences in –SH and -NH mean that irradiation brakes and rearranges the –S-S binding groups; possible starting points for the protein aggregation (Figure 3f). BSA is known to have one –SH group per molecule, the –SH superficial groups per molecule of NP are 37. This suggests aggregation and reorganisation on the structure of the protein molecules forming the NP as it is composed of 2246 BSA molecules [5]. The non-detected –SH might be forming intermolecular S-S stabilising the NP.

The number of NH per BSA (30) and the number of NH detected per nanoparticle (6122), 9% of the total amount of –NH groups (67380) are exposed to the surface (Figure 3f). According to this result, there will be approximately 200 BSA molecules exposed to the surface of the NP. It is possible for the –NH groups of these molecules not to participate in the crosslinking of the BSA of the NP. These groups might be part of the β- sheet-like structures described in the FTIR results (Figure 3b). The increased amount of superficial -NH will ease the covalent binding of a ligand to the NP. Even though the presence of superficial CO is related to protein oxidation [24], it is also a sign of structure alteration due to the irradiation process experimented by the BSA molecules. The CO? also can be forming the β- sheet-like structures described in the FTIR results together with the –NH groups. Therefore, the presence of these groups might be desirable in order to stabilise the BSA NP.

Data collected from spectroscopy experiments showed changes in the UV-Vis absorbance profile of the BSA NP compared to the BSA spectrum. Not all of the albumin molecules forming the NP preserve its structure after protein aggregation (Figure 3a). From the C.D. experiment, protein aggregation was observed in the BSA NP spectrum. This aggregation is due to the desolvation process with ethanol and γ irradiation process (Figure 3e-f). Results in the FT-IR and fluorescence experiments aid the aggregation theory built to explain the signal loss observed in the C.D. experiment (Figure 3b-c). Rohiwal et al., 2016 [22] prepared their BSA NP by desolvation process with a crosslinking method in the presence of glutaraldehyde, and obtained in their FTIR study, a more significant blue shift of the amides I, II and III. The changes observed in Rohiwal et al., 2016 [22] work are observed as frequency displacement to lower frequencies, confirming that structural stability has been changed [22]. The difference between the crosslinking method used here might be the reason for the differences in the spectra obtained. These authors also observed by fluorescence a greater blueshift than observed in our work (c.a.16 nm) [22]. Hence, by using γ irradiation methodology, the BSA structure is more preserved in our NP and loss of function may be prevented.

3.4 Thermogravimetric Analysis (TGA) measurements

TGA measurements showed differences between the BSA and BSA NP degradation profile (Figure 3). The early drop of the curve peaks the NP as a structure more sensitive to heat at

higher temperatures; the sudden weight loss after 300 °C in both samples is due to the loss of molecules such as carbon dioxide and ammonia [25] (Figure 3g). The derivation of each curve states that BSA NP and BSA had a similar behaviour at temperatures lower than 450 ºC, even though there is no displacement of maximum at 295 and 310 ºC in the NP profile in comparison with the BSA profile but values reached were slightly higher in the case of NP than BSA. It can be observed that BSA NP reached after 500 ºC a maximum 12 degrees before BSA and the earlier drop near 0 % of remaining weight (Figure 3h). It is possible that the shift of the maxima at 518 ºC in BSA NP and 530 ºC in BSA was a consequence of preparation process of NP, proteins were slightly affected by irradiation in bonds and conformation as can be seen partially in FT-IR section. This difference is of significance and indicates that the NP involves interactions more prone to be destabilised by heat than BSA.

Differences in thermal degradation between NP and BSA were described by other authors who reported a shift to lower temperatures in thermal degradation, as a sign of protein organisation due to new bonds between albumin molecules [26]. Singh et al. 2017 [27] have reported that degradation (pyrolysis, in nitrogen) became earlier in NP made with BSA concerning control BSA in the range of 250-450 ºC. The reorganisation in structure present in the BSA molecules after the NP preparation process was not only observed by FT-IR, but also by surface characterisation studies. Both suggested the existence of BSA molecule bonding by β sheet-like structures (FT-IR), and the possibility of S-S intermolecular bonds (Figure 3c; 3f). As it is, the T.G.A study in our work confirms the existence of such bonding between albumin molecules during the BSA NP preparation process.

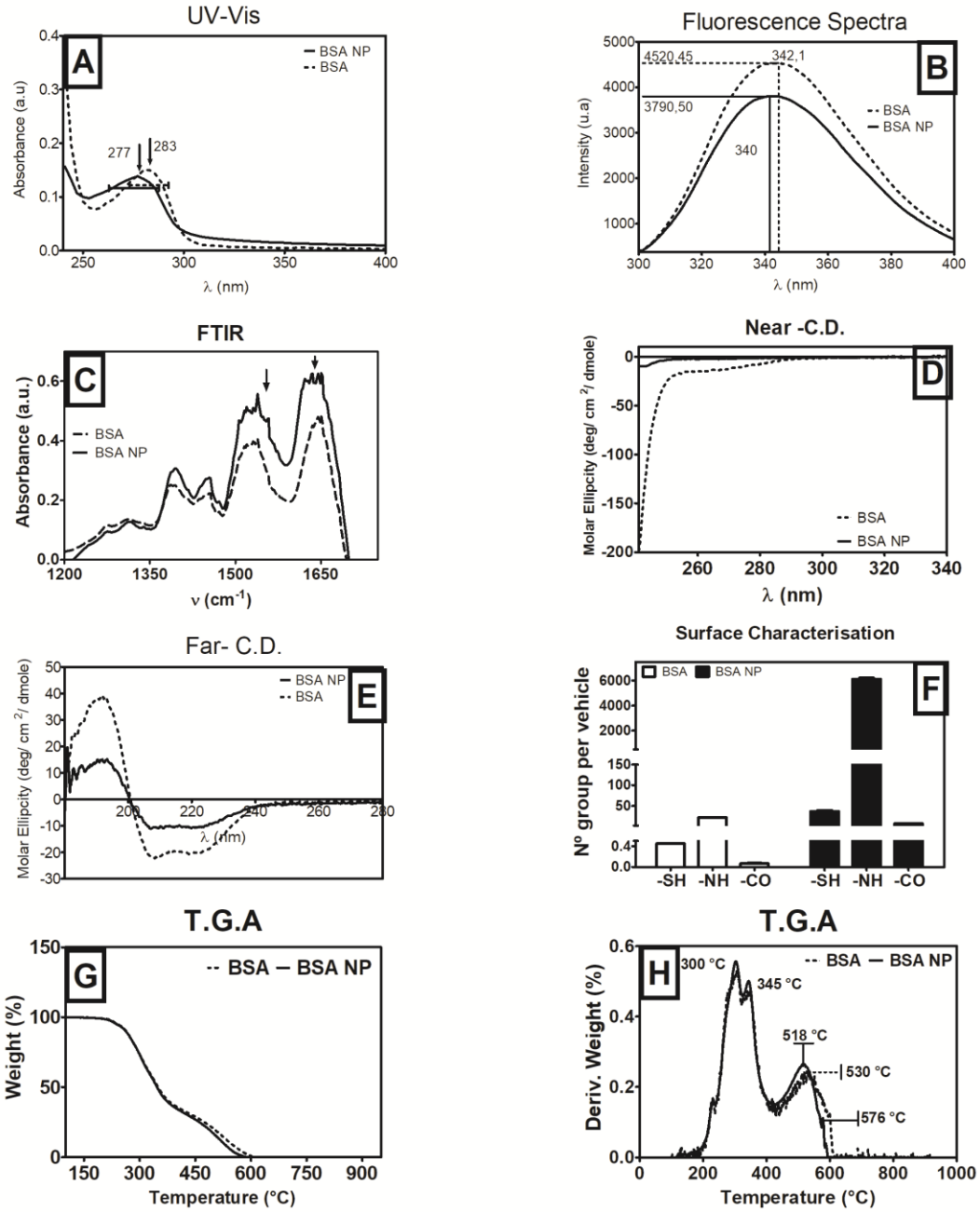

Figure 3. Biophysical studies carried out on the BSA NP; (a) UV-vis spectroscopy profile of BSA (dotted line) and BSA NP (full line)- arrows indicate shoulders´ maxima. (b) FT-IR study of BSA (dotted line) and BSA NP (full line)- _ arrows indicate α- helix maximum and β-sheet-like structures signal (80 scans with a resolution of 1.00 cm^{-1}). (c) Fluorescence study of BSA (dotted line) and BSA NP (full line) _ arrows indicate where the maximum intensity of Trp is set (λex= 295 nm and λem= 377nm; slits: 1.5 nm). C.D. spectroscopy profiles of BSA NP near UV with peaks corresponding to aromatics amino acids (Trp, Tyr, and Phe) (d), and far UV with peaks corresponding to α-helix and β-sheet structures. Experiments correspond to triplicates (e). The surface characterisation for –SH, -NH and –CO groups exposed to the BSA NP surface (f). TGA profile of BSA (dot line) and BSA NP (full line) from 100 – 920 ªC (g). The first derivative of BSA (dot line) and BSA NP (full line) from the data in (g): the central maximum in the first derivative profile are signalled in the figure (h). The data described correspond to duplicates.

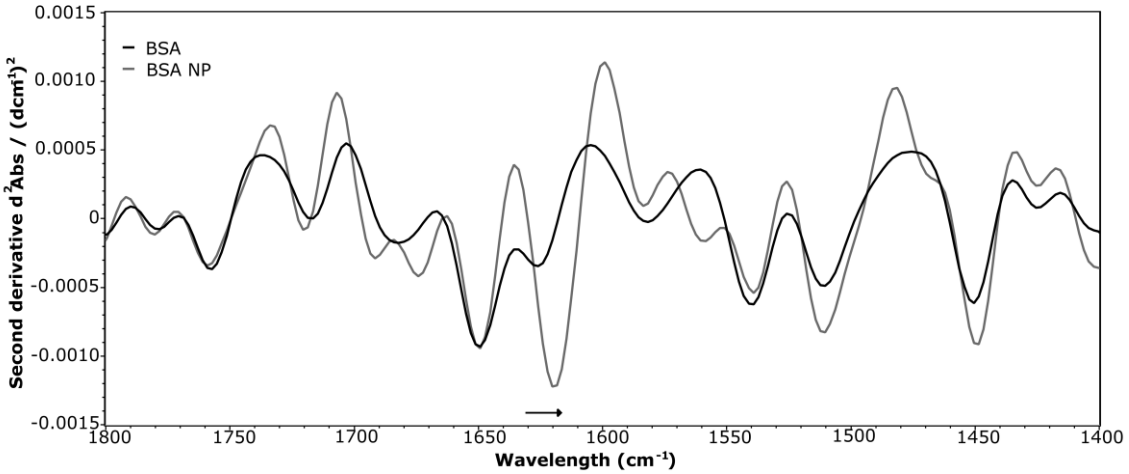

Figure 4 Second derivative treatment of the FT-IR spectra in Figure 3. BSA NP spectra (grey) and BSA (black).

3.5. Folic Acid attachment to the BSA NP

Based on the biophysics characterisation described in this work, we tried to characterise the attachment of folic acid to the BSA NP into folate coated BSA NP (FA-BSA NP). For this purpose, we made use of the BSA NP number of functional surface groups. According to Lee et al., 2009, [28] no further modifications are needed in order to enhance the NP functionality. The possibilities of ligands are such that they could decide the function of the NP for imaging, drug delivery or any other use, providing a more amicable NP to work with than the synthetic manufactured [28]. In our study, folic acid was chosen due to its capacity to enhance the specificity of any NP. Moreover, its attachment to the NP is reproducible and low-cost.

The biophysical characterisation of the FA-NPs showed that the most efficient method for FA decoration of the BSA NP is to attach the ligand to the BSA molecules before NP preparation. Otherwise, the polymers of the FA are at risk of interacting with the Trp of the BSA NP preventing any drug from binding in the main NP binding pocket. Each FA-BSA NP molecule is formed by 2.4 E05 albumin molecules, which result in 6.54 E05 NH groups. Then the totality of the NH groups present in the NP would be attached to an FA molecule or FA polymer (Supplementary Datal).

3.5.1. Interaction study: FA-BSA NP with Emodin (E)

In order to study the FA-BSA NP functionality as a drug delivery system, its interaction with the hydrophobic drug emodin (E) was studied (Figure 5). E has shown in recent years a potential antitumor effect and attempts have been made to diminish its secondary effects by using different drug delivery systems. It was chosen for this study as it also presents the ability to bind to proteins forming complexes [9].

A fluorescence study was carried out in order to estimate the interaction parameters such as dissociation constant (Kd) and maxima drug loading capacity (Bmx) [9] (Figure 5 a-b). The interaction between the FA-BSA NP and E was described by the quenching curve of the tryptophan fluorescence emission of the NP when being incubated with increasing

concentrations of E (Figure 5.a). From the data collected in the experiment, an interaction curve can be represented (Figure 5.b), where a mathematic fitting is done in order to obtain the interaction parameters (Table 1). If Kd is a significant value, then the association constant (Ka) should be small. Therefore, larger values of Kd suggest a low affinity between the NP and drug [9][29]. As it is, FA-BSA NP presents a low value of Kd, which means that the FA-BSA NP has an great affinity for E (Table 1).

According to Sevilla et al., 2007 [9], the Kd for BSA and E varies between 10 e-08 and 10 e-06. In this work, the Kd obtained is in the order 10 e-05, which suggest the affinity is increased because of the derivatisation of the NP. During the preparation process (FA attachment to the BSA and following irradiation), the FA molecules and polymers generate a dense NP. This solid aggregation results in protein structure alteration, increasing the affinity for the E despite the decreased hydrophobic character of the binding pocket (Figure 5a-b). This suggests that the FA-BSA NP has new hydrophobic pockets that are available for the drug to bind with high affinity.

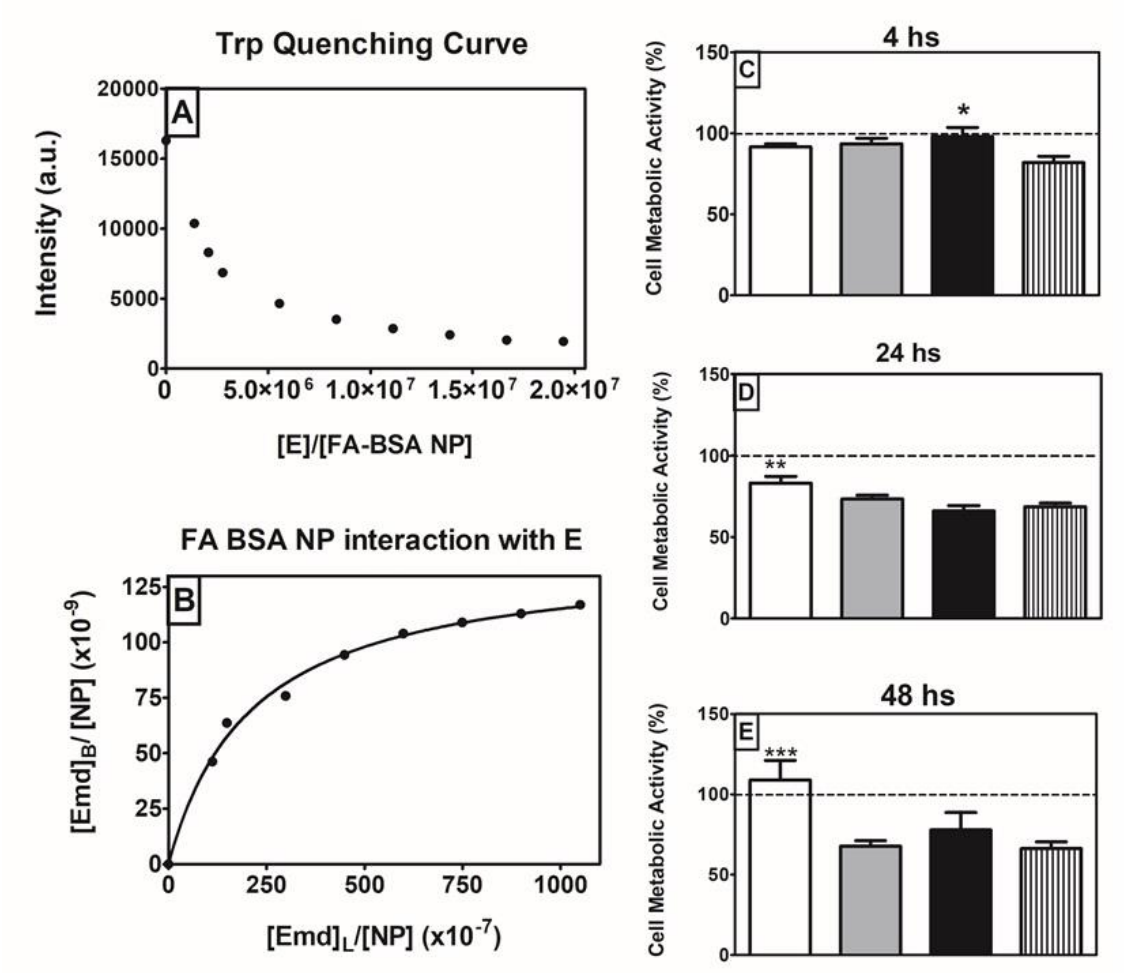

Figure 5 A-B Functionality study of FA-BSA NP as a drug delivery system bound to hydrophobic drug E. (A) Quenching curve of the tryptophan fluorescence emission as E concentration increased. (B) Mathematical fitting was performed with the Scatchard equation [9]. C – E Cytotoxic study in MCF-7 cell line by an MTT test at 4, 24 and 48 h post-FA-BSA NP (white), FA-BSA NPE(grey), and free E incubation (stripe black and white). The 100 % dot line refers to cells without treatment. BSA-NP(black) was also tested as a control to the study.

Table 1 Interaction parameters of the FA-BSA NPE bioconjugate based on the values taken from the mathematical fitting in Figure 2b.

Parameters	FA-BSA NPE
B_{mx}	1,4 e-07 ± 4,2 e-09
K_d	2,1 e-05 ± 2,1 e-06
R^2	0,99

3.5.2. Cytotoxicity study in MCF-7 cells treated with FA-BSA NP

The cytotoxic effect of the FA-BSA NP and the bioconjugate FA-BSA NPE was studied by the effect they had on the cell metabolic activity in the human tumour breast cell line MCF-7. The effects were studied up to 48 hs post incubation, maximum expression of the E effect [29] (Figure 5c-e).

After 4 h of incubation with the different treatments, cells treated with the bioconjugate and FA-BSA NP generate a 10 % decrease in the cell metabolic activity, whereas the cells treated with E generate a 15 % decrease in the cell metabolic activity (Figure 5c-e). At 24 h post incubation, the metabolic activity for cells treated with the bioconjugate and with free E decrease 30 %. However, the metabolic activity for cells treated with FA-BSA NP presents a lesser decrease (15 %). At 48 h post incubation, the cell metabolic activity reaches only 55 % when treated with the bioconjugate and with free E. The FA-BSA NP does not alter the cell metabolic activity 48 h post incubation (Figure 5e).

The cytotoxicity study suggests that while FA-BSA NP is not toxic for the treated cells, the bioconjugate can decrease the cell metabolic activity similarly than the free E can do. Results encourage thinking of the FA-BSA NP as a nanoparticle with great potential as a drug delivery system.

3.6. *Cell immune activation by NPs*

In order to test the ability of NPs to induce an immune response, we incubated immortalised macrophages cell line Raw-Blue with increasing concentration of BSA, BSA NP and FA-BSA NP. We measured the activation of NF-κB, the transcription factor of pro-inflammatory cytokines. BSA monomers induced a weak, but significant NFκB activation whereas both BSA NP and FA-BSA NP induced a stronger activation (Figure 6).

It is believed that there is a connection between the β – sheet percentage in the NP with the activation of a pro-inflammatory response in the cell. The β – sheet structures are involved in the forming of amyloid-like fibres, toxic to the immune system. From the FT-IR study carried out in the different NPs here tested, we were able to observe the presence of such structures in every one of the NPs. These described structures may be the cause of the immune cell response. NPs, in general, are capable of generating two different types of the immune response: (1) they can stimulate it, acting as adjuvants, (2) they can be toxic for the organism [30]. Both, size and physic-chemical structure are responsible for this.

The NF-κB activation by BSA was previously highlighted by Wheeler and co-workers [31]. In our study, molecular albumin induces an immune response in a dose-dependent manner, which is strongly increased when BSA is in aggregate form (Figure 6).

Contrary to Wheeler et al., 2011 [31], in this study a higher diameter (FA-BSA NP 332 nm), does not mean a higher immune response. The reason behind this may be the presence of FA in the NP.

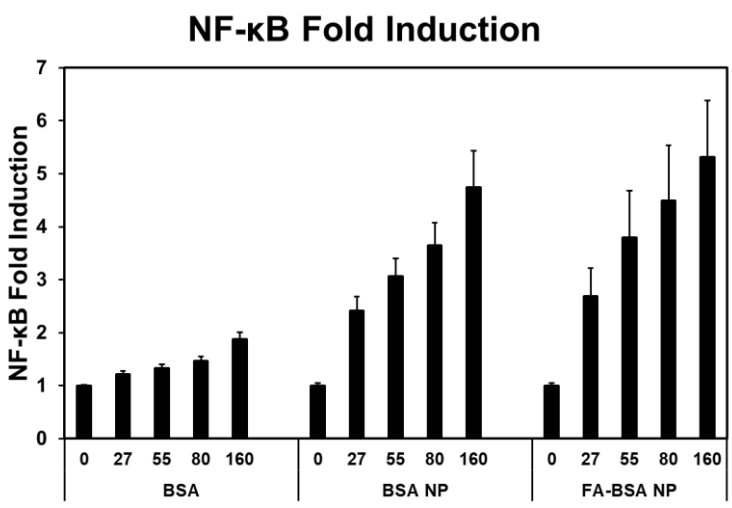

Figure 6 Cell immune response induced by molecular BSA, BSA NP and FA-BSA NP stimuli. Raw-blue cells were incubated for 22 hours with increasing concentrations of molecular BSA, BSA NP and FA-BSA NP and cell supernatants were assayed for NF-κB activation. The bars are the mean of three independent experiments (n=3)

4.0 Conclusion

It was possible to characterise a crosslinked γ-irradiated albumin nanoparticle as a potential novel nanovehicle for drug delivery. Preservation of the primary function of the albumin was observed with enhanced binding efficiency once the NP was formed, as well as an enhanced drug release kinetic profile.

The BSA NP is suitable for attachment with FA, giving a nanoparticle with carrier potential. This nano-delivery system proved to be suitable for hydrophobic antitumoral drugs, maintaining the original molecular properties of the protein but enhancing its delivery features. It has so far proven to be successful against cancerous cells. Moreover, BSA NP activated the NF-κB pathway, suggesting their use as delivery system in vaccine formulation might also serve as an adjuvant to trigger the immune system helping the development of an immune response against the antigen.

The most important finding described in this work is the different NP preparation process by γ-irradiation and BSA-self crosslinking. Compared to the more common desolvation process with a crosslinking method in the presence of glutaraldehyde, with this novel method, the BSA structure is more preserved in the NP and loss of function may be prevented. This improvement may encourage the use of this kind of NP preparation in ongoing research for medical purposes.

5.0 Acknowledgements

This work was supported by grants from Consejo Nacional de Investigaciones Científicas y Técnicas, Universidad Nacional de Quilmes, Ministerio de Ciencia y Tecnología (MINCyT), Comisión de Investigaciones Científicas de la Provincia de Buenos Aires, Nuclear Atomic Energy Agency (IAEA) CRP codes F220064 and F23028.

We are also thankful to Dr Beatriz Patricio from the Institute of Biophysics, Universidade Federal do Rio de Janeiro, Rio de Janeiro, Brazil and to Dr Constanza Flores from Laboratorio de Materiales Biotecnológicos from Universidad Nacional de Quilmes, Bernal, Quilmes, Buenos Aires, Argentina for help with the AFM microscopies. We would also like to thank the FRIA-FNRS (F3/5/5-MCF/XH/FC-17514).

6.0 References

1. Elzoghby, A. O., Samy, W. M., & Elgindy, N. A. (2012). Albumin-based nanoparticles as potential controlled release drug delivery systems. Journal of controlled release, 157(2), 168-182.

2. Estrada, L. H., & Champion, J. A. (2015). Protein nanoparticles for therapeutic protein delivery. Biomaterials science, 3(6), 787-799.

3. Espinoza, S. L. S., Sánchez, M. L., Risso, V., Smolko, E. E., & Grasselli, M. (2012). Radiation synthesis of seroalbumin nanoparticles. Radiation Physics and Chemistry, 81(9), 1417-1421.

4. Achilli, E., Casajus, G., Siri, M., Flores, C., Kadłubowski, S., Alonso, S. D. V., & Grasselli, M. (2015). Preparation of protein nanoparticle by dynamic aggregation and ionizing-induced crosslinking. Colloids and Surfaces A: Physicochemical and Engineering Aspects, 486, 161-171.

5. Siri, M., Grasselli, M., & Alonso, S. D. V. (2016). Albumin-based nanoparticle trehalose lyophilisation stress-down to preserve structure/function and enhanced binding. Journal of pharmaceutical and biomedical analysis, 126, 66-74.

6. Grassetti, D. R., & Murray Jr, J. F. (1967). Determination of sulfhydryl groups with 2, 2′-or 4, 4′-dithiodipyridine. Archives of biochemistry and biophysics, 119, 41-49.

7. Carter, D. C., & Ho, J. X. (1994). Structure of serum albumin. In Advances in protein chemistry (Vol. 45, pp. 153-203). Academic Press.

8. Gelamo, E. L., Silva, C. H. T. P., Imasato, H., & Tabak, M. (2002). Interaction of bovine (BSA) and human (HSA) serum albumins with ionic surfactants: spectroscopy and modelling. Biochimica et Biophysica Acta (BBA)-Protein Structure and Molecular Enzymology, 1594(1), 84-99.

9. Sevilla, P., Rivas, J. M., García-Blanco, F., García-Ramos, J. V., & Sánchez-Cortés, S. (2007). Identification of the antitumoral drug emodin binding sites in bovine serum albumin by spectroscopic methods. Biochimica et Biophysica Acta (BBA)-Proteins and Proteomics, 1774(11), 1359-1369.

10. Pizzuto, M., Lonez, C., Baroja-Mazo, A., Martínez-Banaclocha, H., Tourlomousis, P., Gangloff, M., ... & Bryant, C. (2019). Saturation of acyl chains converts cardiolipin from an antagonist to an activator of Toll-like receptor-4.

11. Davis, S. S. (Ed.). (1984). Microspheres and drug therapy: pharmaceutical, immunological, and medical aspects. Elsevier Publishing Company.

12. Chen, Y. C., Shen, S. C., Lee, W. R., Hsu, F. L., Lin, H. Y., Ko, C. H., & Tseng, S. W. (2002). Emodin induces apoptosis in human promyeloleukemic HL-60 cells accompanied by activation of caspase 3 cascade but independent of reactive oxygen species production. Biochemical pharmacology, 64(12), 1713-1724.

13. Liu, T., Zhang, L., Joo, D., & Sun, S. C. (2017). NF-κB signaling in inflammation. Signal transduction and targeted therapy, 2, 17023.

14. Srinivas, G., Anto, R. J., Srinivas, P., Vidhyalakshmi, S., Senan, V. P., & Karunagaran, D. (2003). Emodin induces apoptosis of human cervical cancer cells through poly (ADP-ribose) polymerase cleavage and activation of caspase-9. European journal of pharmacology, 473(2-3), 117-125.

15. Morris, J. B. (1999). Legume genetic resources with novel “value added” industrial and pharmaceutical use. Perspectives on new crops and new uses, 196-201.

16. Shi, Y., Li, J., Ren, Y., Wang, H., Cong, Z., Wu, G., ... & Zhang, X. (2015). Pharmacokinetics and tissue distribution of emodin loaded nanoemulsion in rats. Journal of drug delivery science and technology, 30, 242-249.

17. Li, Y., Wang, L., Tu, Y., Yan, J., Xu, K., & Li, H. (2015). A new dosage form of emodin: For solubility and dissolution rate enhancement and application in Alzheimer's disease and bacteriostasis. Journal of Drug Delivery Science and Technology, 29, 261-268.

18. Habeeb, A. S. A. (1966). Determination of free amino groups in proteins by trinitrobenzenesulfonic acid. Analytical biochemistry, 14(3), 328-336.

19. Buss, H., Chan, T. P., Sluis, K. B., Domigan, N. M., & Winterbourn, C. C. (1997). Protein carbonyl measurement by a sensitive ELISA method. Free Radical Biology and Medicine, 23(3), 361-366.

20. Du, J., & Hoag, S. W. (2003). Characterization of excipient and tableting factors that influence folic acid dissolution, friability, and breaking strength of oil-and water-soluble multivitamin with minerals tablets. Drug development and industrial pharmacy, 29(10), 1137-1147.

21. Llabot, J. M., de Redin, I. L., Agüeros, M., Caballero, M. J. D., Boiero, C., Irache, J. M., & Allemandi, D. (2019). In vitro characterization of new stabilizing albumin nanoparticles as a potential topical drug delivery system in the treatment of corneal neovascularization (CNV). Journal of Drug Delivery Science and Technology.

22. Rohiwal, S. S., Satvekar, R. K., Tiwari, A. P., Raut, A. V., Kumbhar, S. G., & Pawar, S. H. (2015). Investigating the influence of effective parameters on molecular characteristics of bovine serum albumin nanoparticles. Applied Surface Science, 334, 157-164.

23. Lu, R., Li, W. W., Katzir, A., Raichlin, Y., Yu, H. Q., & Mizaikoff, B. (2015). Probing the secondary structure of bovine serum albumin during heat-induced denaturation using mid-infrared fiberoptic sensors. Analyst, 140(3), 765-770.

24. Grdadolnik, J., & Maréchal, Y. (2001). Bovine serum albumin observed by infrared spectrometry. I. Methodology, structural investigation, and water uptake. Biopolymers: Original Research on Biomolecules, 62(1), 40-53.

25. Levine, R. L., Williams, J. A., Stadtman, E. P., & Shacter, E. (1994). [37] Carbonyl assays for determination of oxidatively modified proteins. In Methods in enzymology (Vol. 233, pp. 346-357). Academic Press.

26. Singh, P., Singh, H., Castro-Aceituno, V., Ahn, S., Kim, Y. J., & Yang, D. C. (2017). Bovine serum albumin as a nanocarrier for the efficient delivery of ginsenoside compound K: preparation, physicochemical characterizations and in vitro biological studies. RSC Advances, 7(25), 15397-15407.

27. Lee, L. A., Niu, Z., & Wang, Q. (2009). Viruses and virus-like protein assemblies—Chemically programmable nanoscale building blocks. *Nano Research*, *2*(5), 349-364.

28. Shi, J., Kantoff, P. W., Wooster, R., & Farokhzad, O. C. (2016). Cancer nanomedicine: progress, challenges and opportunities. Nature Reviews Cancer.

29. Banerjee, M., Pal, U., Subudhhi, A., Chakrabarti, A., & Basu, S. (2012). Interaction of Merocyanine 540 with serum albumins: photophysical and binding studies. Journal of Photochemistry and Photobiology B: Biology, 108, 23-33.

30. Dobrovolskaia, M. A., & McNeil, S. E. (2007). Immunological properties of engineered nanomaterials. Nature nanotechnology, 2(8), 469-478.

31. Wheeler, G. N., & Brändli, A. W. (2009). Simple vertebrate models for chemical genetics and drug discovery screens: lessons from zebrafish and Xenopus. Developmental Dynamics, 238(6), 1287-1308.

Highlights

- By gamma irradiation we achieved a nanoparticle (NP) composed solely of albumin
- Assembly of the NP includes covalent bond, S-S binding and beta-sheet like linkage
- The NP preserves the main function of albumin, while enhancing its binding properties
- A ligand molecule can be attached before gamma irradiation in an effective manner
- The immunogenicity of the NP varies depending on its structure characteristics